



**Intracrystalline incorporation of nacre protein hydrogels  
modifies the mechanical properties of calcite crystals: A  
microcompression study.**

Journal:	<i>Journal of Materials Chemistry B</i>
Manuscript ID	TB-COM-05-2018-001156.R1
Article Type:	Communication
Date Submitted by the Author:	29-May-2018
Complete List of Authors:	Risan, Jared; Bruker Nano Surfaces Jain, Gaurav; New York University, College of Dentistry Pendola, Martin; New York University, Evans, John Spencer; New York University, Laboratory for Chemical Physics

# Intracrystalline incorporation of nacre protein hydrogels modifies the mechanical properties of calcite crystals: A microcompression study.

Jared Risan,<sup>1</sup> Gaurav Jain,<sup>2</sup> Martin Pendola,<sup>2</sup> and John Spencer Evans<sup>2\*</sup>

<sup>1</sup>Nano Surfaces Division, Bruker Corporation, 9625 W. 76<sup>th</sup> Street, Eden Prairie, MN 55344

<sup>2</sup>Laboratory for Chemical Physics, Center for Skeletal and Craniofacial Biology, New York University, 345 E. 24th Street, NY, NY, 10010 USA.

\*To whom correspondence should be addressed: John Spencer Evans, Laboratory for Chemical Physics, Division of Basic Sciences and Center for Skeletal and Craniofacial Medicine, New York University College of Dentistry, 345 E. 24th Street, New York, NY, 10010. Tel.: (212) 998-9605; Fax: (212) 995-4087. Email: [jse1@nyu.edu](mailto:jse1@nyu.edu).

**Electronic Supporting Information:** Comparison of nanoindenter probe size relative to mineral particle size (Figure S1); Displacement controlled compression test (Figure S2); Expansion plots of microcompression stress-strain curves for control, r-AP7, and r-n16.3 samples (Figure S3).

## ABSTRACT

The fracture toughness of mollusk shell nacre has been attributed to many factors, one of which is the intracrystalline incorporation of nacre-specific proteins. Although mechanical force measurements have been made on the nacre layer and on individual calcium carbonate crystals containing occluded organic molecules and macromolecules, there are few if any studies which examine the impact of occluded proteins on the mechanical properties of calcium carbonate crystals. To remedy this, we performed microcompression studies of calcite crystals grown in the presence and absence of two recombinant nacre proteins, r-AP7 (*H. rufescens*, intracrystalline proteome) and r-n16.3 (*P. fucata*, framework proteome), both of which are known aggregators that form hydrogel nanoinclusions within *in vitro* calcite. We find that, relative to protein-free calcite, the intracrystalline inclusion of either r-AP7 or r-n16.3 nacre protein hydrogels within the calcite crystals leads to a reduction in strength. However, nacre protein – modified crystals were found to exhibit elastic deformation under force compared to control scenarios, with no discernable differences noted between intracrystalline or framework protein-modified crystals. We conclude from our *in vitro* microcompression studies that the intracrystalline incorporation of nacre proteins can contribute to fracture-resistance of the crystalline phase by significantly reducing both modulus AND critical strength

## INTRODUCTION

The creation of protective invertebrate calcium carbonate skeletal elements such as the mollusk shell nacre require the assembly of mineral nanoparticles into mesoscale crystals.<sup>1-4</sup> This process is aided by specific matrix proteins<sup>5,6</sup> which guide the nucleation process and subsequent particle assembly via the formation of protein hydrogel phases that modulate hydration and ion sequestration.<sup>7,8</sup> Ultimately, as the mineral nanoparticles form, there are a number of proteins or other biomacromolecules which become randomly occluded within calcium carbonate crystals, typically at low weight percent.<sup>9-11</sup> This incorporation affects the texture, lattice strain, and anisotropy of the crystal and promote fracture toughness.<sup>12-14</sup> It is believed that this intracrystalline incorporation process initiates at the amorphous calcium carbonate (ACC) mineral precursor stage that precedes crystalline transformation.<sup>15,16</sup> Additives, such as proteins, associate with or stabilize ACC and become incorporated into the mineral phase during the amorphous-to-crystalline transformation process.<sup>10,11,17,18</sup> To monitor this process a number of *in vitro* mineralization systems have been developed wherein additives such as amino acids,<sup>19-21</sup> agarose gels,<sup>22</sup> recombinant nacre proteins,<sup>11</sup> and polymers<sup>23-25</sup> have been successfully incorporated into calcium carbonates. These experiments confirm that a wide variety of molecular and macromolecular organic species can be randomly incorporated within crystals with subsequent modifications of the physical properties of these crystals.<sup>11,19-25</sup> However, the phenomenon of intracrystalline modifications by *biomineralization proteins* is still poorly understood and thus our ability to develop novel organic-occluded inorganic materials is limited.

Much of our current understanding of protein-created intracrystalline nanovoids and their formation comes from *in vitro* calcite model studies<sup>26-28</sup> that utilized recombinant mollusk shell nacre-specific proteins. These experiments allowed reproducibility and monitored the random

deposition of protein hydrogels onto existing calcite crystals that formed within micromineralization assays.<sup>26-28</sup> Two of these proteins, the Pacific red abalone nacre intracrystalline AP7 (66 AA, 7565 Da)<sup>26,27</sup> and the Japanese pearl oyster framework n16.3 (108 AA, 12947 Da)<sup>28</sup> were found to occlude within the peripheral subsurface regions of calcite over a 30-60 min period, creating randomly-distributed nanoporosities and nanochambers within the crystals as well as surface nanotexturing (Figure 1).<sup>26-28</sup> However, the material properties of these protein-modified crystals were not investigated at the time, and thus potential strengthening or weakening effects that these proteins have on calcium carbonate crystals are not yet known.

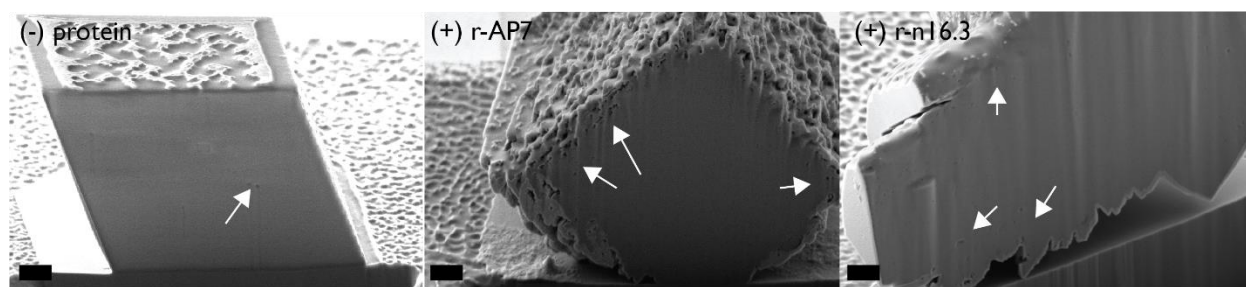


Figure 1. SEM images of focused ion beam (FIB) sectioned calcite crystals obtained from control (protein-free) and r-AP7, r-n16.3 mineralization assays. White arrows indicate location of hydrogel inclusions. Scalebars = 200 nm. Adapted from references 17,18.

To arrive at a better understanding of intracrystalline protein occlusion and resultant crystal material properties, we embarked on a microcompression study (stress-strain) of calcite crystals produced in calcite-based micromineralization assays in the presence and absence of recombinant AP7 (r-AP7)<sup>29</sup> and n16.3 (r-n16.3).<sup>30</sup> Note that we chose the calcite-based assay to be consistent with the assays utilized in our earlier nacre protein hydrogel studies of intracrystalline incorporation<sup>27,28</sup> as well as the assays employed in polymer incorporation nanoindentation studies.<sup>11,19-25</sup> This study is innovative in that we are mechanically testing specific crystals generated by hydrogelator proteins that are representatives of two nacre-regulating proteomes that are expressed within different regions of the nacre tablets (AP7 = intracrystalline within the tablets;<sup>29</sup> n16.3 = framework layer surrounding the tablets<sup>30</sup>). The results were interesting: regarding average

loading, crystals that form in the absence of protein possessed the highest critical stress compared to crystals generated in the presence of either nacre protein. In terms of average strain, the control, r-AP7, and r-n16.3 crystals were found to be statistically equivalent. However, the most dramatic finding was the stiffness values: here, compared to the control crystals, r-AP7 and r-n16.3 modified crystals had reduced average stiffness and exhibited higher strain under load. Thus, the protein intracrystalline inclusions introduced into *in vitro* calcite crystals yields modified material properties, with an emphasis on a reduced stiffness, which may be important for creating regions of elastic deformability within the nacre layer.<sup>31-33</sup>

## EXPERIMENTAL

*Recombinant protein expression and purification.* The bacterial expression and purification of r-AP7 and r-n16.3 were achieved using the protocols described in our earlier studies.<sup>29,30</sup> Lyophilized proteins were dissolved in 30 nm ultrapure Fisher Molecular Biology grade water (Fisher Scientific, USA) to create stock solutions for subsequent use.

*In vitro micro-mineralization assays.* Calcite-specific mineralization microassays were conducted by mixing equal volumes of 20 mM  $\text{CaCl}_2 \cdot 2\text{H}_2\text{O}$  (pH 5.5) and 20 mM  $\text{NaHCO}_3 / \text{Na}_2\text{CO}_3$  buffer (pH 9.75 in 30nm filtered ultrapure Molecular Biology-grade water )(Fisher Scientific, USA) to a final volume of 500  $\mu\text{L}$  in sealed polypropylene tubes and incubating at room temperature for 1 hr.<sup>26-30</sup> The final pH of the reaction mixture was measured and found to be approximately 8.0 - 8.2.<sup>26-30</sup> Individual aliquots of r-n16.3 and r-AP7 stock solutions were added to the calcium solution prior to the beginning of the reaction, with final assay concentrations of each protein to be 10  $\mu\text{M}$ . Mineral and protein deposits formed during all assays were captured on 5 x 5 mm Si

wafer chips (Ted Pella, Inc.) that were placed at the bottoms of the vials. Upon completion of the mineralization assay period, the Si wafers were rinsed thoroughly with calcium carbonate saturated methanol and dried overnight at room temperature prior to analysis.<sup>26-30</sup>

Microcompression measurements. Nanoindentation load-displacement and stiffness measurements of control and r-AP7, r-n16.3-associated calcite crystals were made using a Bruker TI980 Triboindenter equipped with a multirange transducer. The mounting of crystals was accomplished by epoxying each mineral-coated Si wafer to an AFM puck with Loctite 495, and magnetically securing the puck to the stage. The size of the flat punch probe relative to mineral particle size was determined using a single crystal aluminum metal substrate and then compared to actual particle size (Figure S1, Electronic Supporting Information). The displacement-controlled compression test involved increasing the displacement linearly at 200 nm/sec until the particle failed or the substrate was contacted (Figure S2, Electronic Supporting Information). The corresponding critical load and critical displacement to cause failure was recorded. Additionally, stiffness measurements were calculated for particles that showed linear force–displacement behavior before failure. Displacement controlled indentation tests were performed using a multirange transducer equipped with a flat punch probe (20  $\mu\text{m}$  diameter, 60° conical diamond flat punch) to measure critical stress and strain of selected crystals to cause microcrystal fracture. Stress,  $\sigma$ , and strain,  $\varepsilon$ , were determined as<sup>34,35</sup>

$$\sigma = \frac{P}{l^2}, \quad \varepsilon = \frac{\Delta l}{l} \quad \text{Eq. 1}$$

Where  $l$  is the average lengths of the sides of the top, and  $P$  is the applied load. For this analysis, the particles are assumed to be cubic, which from Figure S2 (Electronic Supporting Information) is a close approximation for rhombohedral calcite crystals. The displacement-controlled

compression test<sup>35,36</sup> involved increasing the displacement linearly at 200 nm/s until the crystal failed or the substrate was contacted. The corresponding critical load and critical displacement to cause failure was recorded. Additionally, stiffness measurements<sup>34,35</sup> of the initial loading portion were calculated for crystals that showed linear force–displacement behavior prior to failure. All measurements were performed on 10 individual crystals for each sample.

## RESULTS AND DISCUSSION

We note that microcompression studies have been performed on calcite crystals, including calcite that possesses organic inclusions. These studies have shown that the incorporation of amino acids,<sup>19,21</sup> copolymer micelles,<sup>23</sup> and copolymer worms<sup>24</sup> into calcite crystals yields increased hardness which is consistent with the findings for protein-occluded biogenic calcite obtained from mollusk shells. In contrast, nanoindentation studies of the mollusk shell reveal that the void-containing aragonite platelets are more ductile and less stiff than non-biogenic calcium carbonates.<sup>32</sup> These results suggest that the crystal mechanical properties induced by occluded species can vary to some extent. In this current study, we examine the effects of individual, purified recombinant nacre proteins (r-AP7, r-n16.3) on *in vitro* calcite material properties using stress-strain and stiffness measurements relative to control, protein-free scenarios.

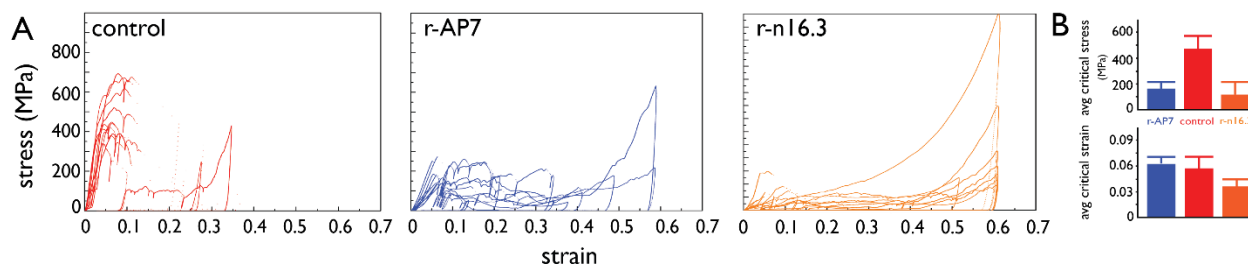


**Figure 2.** (A) Microcompression stress-strain curves obtained for control, r-AP7, and r-n16.3 calcite crystals ( $n = 10$ ). (B) Histogram plots of the < average > critical stress and critical strain values ( $\pm$  S.D.) that cause crystal failure ( $n = 10$ ).

In Figure 2A, we present the stress-strain curves (Eq. 1) obtained for calcite crystals recovered from protein-free, r-AP7, and r-n16.3 micromineralization assays (see also Figure S3,



Electronic Supporting Information, expansion plots), along with the average critical stress and strain values (Figure 2B). These curves provide a “mechanical fingerprint” of a materials response to microcompression.<sup>34,35</sup> As shown in Figure 2A, there is a great degree of variation in the critical stress-strain values obtained for individual crystals in each sample category. We suspect that this variation arises from the microstructural heterogeneity of these samples, particularly those of r-AP7 and r-n16.3, which contain randomly distributed nanoporosities of varying sizes (Figure 1).<sup>26-</sup>  
<sup>28</sup> We found that the control calcite sample possessed the highest critical stress by a factor of 2-3x over that of the protein-modified crystals (Figure 2B). This indicates that the intracrystalline inclusion of nacre protein hydrogels within the calcite crystals leads to a reduction in strength. Most likely this is due to the presence of multiple nanoporosities near the surface of r-AP7 and r-n16.3 calcite crystals (Figure 1),<sup>26-28</sup> which would be expected to fail upon compression compared to control calcite crystals which possess few if any subsurface porosities. This result is what one would expect from a simple Griffith flaw size criterion in a brittle solid.<sup>34-36</sup> Interestingly, the control and protein samples tested as being nearly statistically equivalent in average strain values (Figure 2B), with r-n16.3 exhibited strain values that were ~20% lower compared to the control and r-AP7 samples. These findings are like those obtained for nacre aragonite tablets taken from mollusk shells, where it was discovered that there was more material collapse and pile-up from indentation compared to non-biogenic crystals.<sup>37</sup>

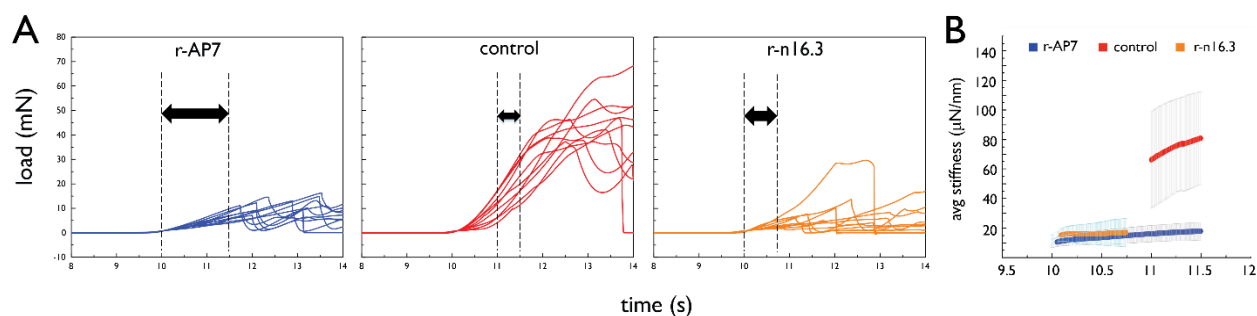


**Figure 3.** (A) Plots of nanoindentor load as a function of time for the three samples ( $n = 10$ ). (B) <Average> stiffness values ( $\pm$  S.D.). Data within the arrow regions in (A) was used to calculate the values in (B).

We next examined the elastic deformation or stiffness parameter<sup>34-36</sup> for each sample crystal collection (Figure 3A, B). The stiffness curves clearly exhibit differences, with the control samples possessing the highest stiffness values (by a factor of 4x) relative to the r-AP7 and r-n16.3 crystals that are nearly equivalent as a function of time (Figure 3B). Proving whether there are regions of pure elasticity or pure ductility in any of the nacre protein-modified crystals is not within the scope of this paper. Nonetheless, these results indicate that the calcite crystals modified by the nacre proteins have a significantly reduced modulus AND critical strength. Thus, unlike other organic intracrystalline additives, nacre proteins do not increase the strength of calcite; rather, they decrease it, and this finding is consistent with increased plasticity or elastic deformation characteristics noted for protein-impregnated aragonite tablets.<sup>32,33,37-40</sup>

## CONCLUSIONS

In summary, our microcompression study is a first-time examination of the effects of individual nacre biomineralization proteins on the material properties of calcium carbonate crystals. We note that calcite crystals generated in the presence and absence of recombinant nacre proteins r-AP7 (intracrystalline) and r-n16.3 (framework) reveals that the representatives of each proteome are nearly equivalent in their ability to modify the material properties of *in vitro* calcite crystals. Compared to unmodified calcite crystals, nacre protein-modified crystals are less resistant to microcompression forces (Figure 2A, B), and these same protein-modified calcite crystals are nearly equivalent to the unmodified calcite crystals regarding strain (Figure 2B). These properties most likely arise because of protein hydrogel incorporation within subsurface nanoporosities within these crystals (Figure 1), which give way under stress. Again, this is consistent with other nanoindentation studies performed on the bulk nacre layer<sup>32,33</sup> as well as the nacre tablets themselves,<sup>37-40</sup> which were found to possess increased plastic deformation. Further, we note that

the mechanical response of organic additive-modified calcite is lower in strength compared to untreated calcite crystals.<sup>21-25</sup> Thus, the force measurements obtained for nacre and aragonite tablets reflect the unique material behavior of protein hydrogel nanoinclusions within the crystalline phase of the mineral.

The most surprising aspect of this study was the stiffness response of calcite crystals (Figure 3), wherein nacre protein – modified crystals were found to possess significantly reduced modulus or increased elastic deformation compared to control scenarios, with no discernable differences noted between intracrystalline or framework protein-modified crystals. This suggests that the nacre protein hydrogel nanoinclusions, regardless of their proteomic origin, create a calcite crystal that is reduced in stiffness. Again, this data correlates with the force studies conducted on nacre and aragonite tablets, both of which demonstrated reduced modulus response as well.<sup>32,33,37-40</sup> Our findings have profound material implications for aragonite tablets: we speculate that the immediate crystalline environment around randomly distributed protein hydrogel nanoinclusions could conceivably deform under force, thus preventing catastrophic failure of the remaining bulk crystalline material. We await further *in situ* and *in vitro* investigations of the mollusk nacre layer and associated proteins which can ascertain this possibility.

## **CONFLICTS OF INTEREST**

There are no conflicts to declare.

## **ACKNOWLEDGEMENTS**

We thank Dr. Douglas Stauffer, Bruker Corporation, for his help with this manuscript. Portions of this research (mineralization assays, SEM/FIB imaging) was supported by the U.S. Department of Energy, Office of Basic Energy Sciences, Division of Materials Sciences and Engineering under

Award DE-FG02-03ER46099. This report represents contribution number 93 from the Laboratory for Chemical Physics, New York University.

## REFERENCES

1 Zhang, G., Li, X. Uncovering aragonite nanoparticle self-assembly in nacre – A natural armor. *Crystal Growth and Design* 2012, **12**, 4306-4310.

2 DeVol, R.T., Sun, C.Y., Marcus, M.A., Coppersmith, S.N., Myneni, S.C.B., Gilbert, P.U.P.A. Nanoscale transforming mineral phases in fresh nacre. *J. Am. Chem. Soc.* 2015, **137**, 13325-13333.

3 Hovden, R., Wolf, S.E., Holtz, M.E., Marin, F., Muller, D.A., Estroff, L.A. Nanoscale assembly processes revealed in the nacre-prismatic transition zone of *Pinna nobilis* mollusk shells. *Nature Commun.* 2015, **6**, 10097-10105.

4 Zheng, G., Xu, J. From colloidal nanoparticles to a single crystal: New insights into the formation of nacre's aragonite tablets. *J. Struct. Biol.* 2013, **182**, 36-43.

5 Zhang, G., Fang, X., Guo, X., Li, L., Luo, R., Xu, F., Yang, P., Zhang, L., Wang, X., Qi, H., Xiong, Z., Que, H., Xie, Y., Holland, P.W.H., Wang, X., Paps, J., Zhu, Y., Wu, F., Chen, Y., Wang, J., Peng, C., Meng, J., Yang, L., Liu, J., Wen, B., Zhang, N., Huang, Z., Zhu, Q., Feng, Y., Mount, A., Hedgecock, D., Xu, Z., Liu, Y., Domazet-Loso, T., Du, Y., Sun, X., Zhang, S., Liu, B., Cheng, P., Jiang, X., Li, J., Fan, D., Wang, W., Fu, W., Wang, T., Wang, B., Zhang, J., Peng, Z., Li, Y., Li, N., Wang, J., Chen, M., He, Y., Tan, F., Song, X., Zheng, Q., Huang, R., Yang, H., Du, X., Chen, L., Yang, M., Gaffney, P.M., Wang, S., Luo, L., She, Z., Ming, Y., Huang, W., Zhang, S., Huang, B., Zhang, Y., Qu, T., Ni, P., Miao, G., Wang, W., Zhang, S., Haung, B., Zhang, Y., Qu, T., Ni, P., Miao, G., Wang, J., Wang, Q., Steinberg, C.E.W., Wang, H., Li, N., Qian, L., Zhang, G., Li, Y., Yang, H., Liu, X., Wang, J., Yin, Y., Wang, J., The oyster genome reveals stress adaptation and complexity of shell formation. *Nature* 2012, **490**, 49-54.

6 Liu, X., Li, J., Xiang, L., Sun, J., Zheng, G., Zhang, G., Wang, H., Xie, L., Zhang, R. The role of matrix proteins in the control of nacreous layer deposition during pearl formation. *Proc. R. Soc. B* 2012, **279**, 1000-1007.

7 Pendola, M., Evans, J.S. Non-invasive  $\mu$ CT visualization of mineralization directed by sea urchin- and nacre-specific proteins. *Crystal Growth and Design* 2018, **18**, 1768-1775.

8 Pendola, M., Evans, J.S. Insights into mollusk shell formation: Interlamellar and lamellar specific nacre protein hydrogels differ in ion interaction signatures. *J. Phys. Chem B* 2018, **122**, 1161-1168.

9 Gries, K., Kröger, R., Kübel, C., Fritz, M., Rosenauer, A. Investigation of voids in the aragonite platelets of nacre. *Acta Biomaterialia* 2009, **5**, 3038-3044.

10 Aizenberg, J., Hanson, J., Koetzle, T.F., Weiner, S., Addadi, L. Control of macromolecular distribution within synthetic and biogenic single crystal calcite. *J. Am. Chem. Soc.* 1997, **119**, 881-886.

- 11 Weber, E., Bloch, L., Guth, C., Fitch, A.N., Weiss, I.M., Pokroy, B. Incorporation of a recombinant biomineralization fusion protein into the crystalline lattice of calcite. *Chem. Mat.* 2014, **26**, 4925-4932.
- 12 Younis, S., Kauffmann, Y., Bloch, L., Zolotoyabko, E. Inhomogeneity of nacre lamellae on the nanometer length scale. *Cryst. Growth and Design* 2012, **12**, 4574-4579.
- 13 Pokroy B., Fitch A.N., Lee, P.L., Quintana, J.P., Caspi, E.N., Zolotoyabko, E. Anisotropic lattice distortions in the mollusk-made aragonite: a widespread phenomenon. *J. Struc. Biol.* 2006, **153**, 145-150.
- 14 Li, H.Y., Xin, H.L., Kunitake, M.E., Keene, E.C., Muller, D.A., Estroff, L.A. Calcite prisms from mollusk shells (*Atrina rigida*): swiss-cheese-like organic-inorganic single-crystal composites. *Adv. Funct. Mater.* 2011, **21**, 2028-2034.
- 15 DeVol, R.T., Sun, C.Y., Marcus, M.A., Coppersmith, S.N., Myneni, S.C.B., Gilbert, P.U.P.A. Nanoscale transforming mineral phases in fresh nacre. *J. Am. Chem. Soc.* 2015, **137**, 13325-13333.
- 16 Hovden, R., Wolf, S.E., Holtz, M.E., Marin, F., Muller, D.A., Estroff, L.A. Nanoscale assembly processes revealed in the nacreprismatic transition zone of *Pinna nobilis* mollusk shells. *Nature Commun.* 2015, **6**, 10097-10105.
- 17 Gower, L.B. Biomimetic model systems for investigating the amorphous precursor pathway and its role in biomineralization. *Chem. Rev.* 2008, **108**, 4551-4627.
- 18 Goodwin, A.L., Michel, F.M., Phillips, B.L., Keen, D.A., Dove, M.T., Reeder, R.J. Nanoporous structure and medium-range order in synthetic amorphous calcium carbonate. *Chem. Mat.* 2010, **22**, 3197-3205.
- 19 Borukhin, S., Bloch, L., Radlauer, T., Hill, A.H., Fitch, A.N., Pokroy, B. Screening the incorporation of amino acids into an inorganic crystal host: the case of calcite. *Adv. Materials.* 2012, **22**, 4216-4224.
- 20 Brif, A., Ankonina, G., Drathen, C., Pokroy, B. Semiconductors: Bio-inspired band gap engineering of zinc oxide by intracrystalline incorporation of amino acids. *Adv. Materials.* 2014, **26**, 477-481.
- 21 Kim, Y.Y., Carloni, J.D., Demarchi, B., Sparks, D., Reid, D.G., Kunitake, M.E., Tang, C.C., Duer, M.J., Freeman, C.L., Pokroy, B., Penkman, K., Harding, J.H., Estroff, L.A., Baker, S.P., Meldrum, F.C. Tuning harness in calcite by incorporation of amino acids. *Nature Materials* 2016, **15**, 902-910.
- 22 Li, H.Y., Xin, H.L., Muller, D.A., Estroff, L.A. Visualizing the 3D internal structure of calcite single crystals grown in agarose hydrogels. *Science* 2009, **326**, 1244-1247.
- 23 Kim, Y.Y., Ganesan, K., Yang, P., Kulak, A.N., Borukhin, S., Pechook, S., Ribeiro, L., Kroger, R., Eichhorn, S.J., Armes, S.P., Pokroy, B., Meldrum, F.C. An artificial biomineral formed by incorporation of copolymer micelles in calcite crystals. *Nature Materials* 2011, **10**, 890-896.

- 24 Kim, Y.Y., Semsarilar, M., Carloni, J.D., Cho, K.R., Kulak, A.N., Polishchuk, I., Hendley, C.T., Smeets, P.J.M., Fielding, L.A., Pokroy, B., Tang, C.C., Estroff, L.A., Baker, S.P., Armes, S.P., Meldrum, F.C. Structure and properties of nanocomposites formed by the occlusion of block copolymer worms and vesicles within calcite crystals. *Adv. Materials* 2016, **26**, 1382-1392.
- 25 Ning, Y., Fielding, L.A., Ratcliffe, L.P.D., Wang, Y.W., Meldrum, F.C., Arms, S.P. Occlusion of sulfate-based deblock copolymer nanoparticles within calcite: Effect of varying the surface density of anionic stabilizer chains. *J. Am. Chem. Soc.* 2016, **138**, 11734-11742.
- 26 Chang, E.P., Williamson G., Evans, J.S. Focused ion beam tomography reveals the presence of micro-, meso-, and macroporous intracrystalline regions introduced into calcite crystals by the gastropod nacre protein AP7. *Crystal Growth and Design* 2015, **15**, 1577-1582.
- 27 Chang, E.P., Russ, J.A., Verch, A., Kroeger, R., Estroff, L.A., Evans, J.S. Engineering of crystal surfaces and subsurfaces by an intracrystalline biomineralization protein. *Biochemistry* 2014, **53**, 4317-4319.
- 28 Chang, E.P., Russ, J.A., Verch, A., Kroeger, R., Estroff, L.A., Evans, J.S. Engineering of crystal surfaces and subsurfaces by framework biomineralization protein phases. *Cryst.Eng. Commun.* 2014, **16**, 7406-7409.
- 29 Perovic, I., Chang, E.P., Verch, A., Rao, A., Cölfen, H., Kroeger, R., Evans, J.S. An oligomeric C-RING nacre protein influences pre-nucleation events and organizes mineral nanoparticles. *Biochemistry* 2014, **53**, 7259-7268.
- 30 Perovic, I., Chang, E.P., Lui, M., Rao, A., Cölfen, H., Evans, J.S. A framework nacre protein, n16.3, self-assembles to form protein oligomers that participate in the post-nucleation spatial organization of mineral deposits. *Biochemistry* 2014, **53**, 2739-2748.
- 31 Jackson, D.J., Reim, L., Randow, C., Cerveau, N., Degnan, B.M., Fleck, C. Variations in orthologous shell-forming proteins contribute to molluscan shell diversity. *Mol. Biol. Evol.* 2017, **34**, 2959-2969.
- 32 Li, X., Chang, W.C., Chao, Y.J., Wang, R., Chang, M. Nanoscale structural and mechanical characterization of a natural nanocomposite material: The shell of the red abalone. *Nano Letters* 2004, **4**, 613-617.
- 33 Schneider, A.S., Heiland, B., Peter, N.J., Guth, C., Arzt, E., Wiess, I.M. Hierarchical superstructure identified by polarized light microscopy, electron microscopy and nanoindentation: implications for the limits of biological control over the growth mode of abalone sea shells. *BMC Biophysics* 2012, **5**, 1-12.
- 34 Hainsworth, S.V., Chandler, H.W., Page, T.F. Analysis of nanoindentation load-displacement loading curves. *J. Materials Res.* 1996, **11**, 1987-1995.
- 35 Tracy, C., A compression test for high strength ceramics. *Journal of Testing and Evaluation*, 1987, **15**, 14-19.

36 Gong, J., Peng, Z., Miao, H. Analysis of the nanoindentation load-displacement curves measured on high-purity fine-grained alumina. *J. Eur. Ceramic Soc.* 2005, **25**, 649-654.

37 Nanoscale morphology and indentation of individual nacre tablets from the gastropod mollusk *Trochus niloticus*. *J. Mat. Res.* 2005, **20**, 2400-2419.

38 Barthelat, F., Li, C.M., Comi, C., Espinosa, H.D. Mechanical properties of nacre constituents and their impact on mechanical performance. *J. Mat. Res.* 2006, **21**, 1977-1986.

39 Moshe-Drezner, H., Shilo, D., Dorogoy, A., Zolotoyabko, E. Nanometer-scale mapping of elastic modulus in biogenic composites: The nacre of mollusk shells. *Adv. Mat.* 2010, **20**, 2723-2728.

40 Kearney, C., Zhao, Z., Bruet, B.J.F., Radovitzky, R., Boyce, M.C., Ortiz, C. Nanoscale anisotropic plastic deformation in single crystal aragonite. *Phys. Rev. Lett.* 2006, **96**, 255505-255509.

Table of Contents Figure

